

APPROACHES IN MODELLING A WAVEGUIDE RF-LINAC THz-FEL

Yu. Lurie*, Y. Pinhasi, Ariel University Center of Samaria, Ariel, Israel
 M. Tecimer, NHMFL / Florida State University, Tallahassee, FL 32310, USA

Abstract

A widely used approach in describing radiation fields generated by short pulse rf linac FEL oscillators is based on modal expansion of the intracavity fields and solving the wave equation for the amplitudes of the excited transverse cavity eigenmodes, in time and axial dimension. In this time domain approach, mode amplitudes are calculated by adopting the slowly varying envelope approximation (SVEA). The longitudinal propagation number k_z of the carrier wave is usually assumed to represent a group velocity and a wave impedance of the frequencies encompassed within the spectral bandwidth of the optical pulse envelope as it evolves within the interaction region. However, in cases where dispersive effects arising from a waveguided cavity become influential, the space-frequency approach is a straightforward method to tackle the problem without introducing further approximations. One such case is being studied based on a highly slippage dominated short pulse rf-linac FEL operating at long wavelengths.

INTRODUCTION

The aim of this paper is to present numerical design tools for investigating the temporal and spectral characteristics of THz pulses generated by short pulse rf-linac based waveguided FEL oscillators. We demonstrate application of these numerical tools on the design study and parameter optimization of a THz FEL system that is expected to operate over a frequency range between 100-1100 microns [1]. Combination of effects resulting from the use of picoseconds short electron pulses and long radiation wavelengths spread over such a wide spectral range on the one hand and propagation of short radiation pulses in lengthy waveguide resonators (as required in most of the rf-linac driven FELs) on the other hand, necessitate a careful analysis of the interplay between enhanced coherent spontaneous emission (CSE), waveguide dispersion (group velocity dispersion), slippage and cavity desynchronisation effects. In devising the numerical design tool, we adopt space-frequency approach [2, 3] which enables a correct description of these effects but it is time consuming when simulating an oscillator FEL configuration. On the other hand, employing an additional formalism to model the relevant aspects of the problem in an approximated way while creating practical means in terms of cpu usage. The former rigorous formalism is used to validate the application range of the latter in tackling the design problem with a reasonable accuracy

and replace it in cases of shortcomings in modelling properly the physics of the above mentioned THz FEL system. The two methods presented in the paper are contemplated for the design study of the planned wide spectral range, long wavelength, short pulse waveguide THz-FEL oscillator.

Sample results are given applying the developed formalisms on a highly slippage dominated FEL regime where submillimeter to millimeter wavelength radiation is generated by a few picoseconds long high peak current electron bunches.

DESCRIPTION OF THE MODELS

Time domain model

The time domain approach presented here and the implemented numerical algorithm is described in details in [4, 5]. Several assumptions are adopted in the model that reduce greatly the computational effort in order to enable an optimization of the system parameters. The longitudinal motion of each macroparticle is tracked whereas the transverse motion is accounted for by the beam envelope equations [4]. The latter includes the influence of 3D beam effects in an averaged manner. The profile of the optical field is defined by the transverse modes that are excited in a parallel plate (PP) waveguide resonator [5, 6]. The evolution of the mode amplitudes is governed by Eq. (1) where, by adopting SVEA and introducing the transformations $z' = z - v_g t$ and $\bar{z} = z - v_z t$, the inhomogeneous wave equation simplifies into:

$$\frac{\partial}{\partial z} u_q(z, z') = j \frac{f_b \mathbf{F} A_{u0}}{2k_{zq}} \cdot \frac{\omega_p^2}{c^2} \\ \times \zeta_q(z, \bar{z}) \frac{\chi(z, \bar{z})}{N_{\bar{z}}(z, \bar{z})} \sum_i^{N_{\bar{z}}(z, \bar{z})} e^{-j\theta_{iq}(z, \bar{z})} \quad (1)$$

In (1) $u_q(z, z')$ is the complex envelope of a modulated wave train with carrier frequency ω and axial wavenumber k_{zq} of the excited q 'th mode, which satisfy the waveguide dispersion relation. $\theta_{iq}(z, \bar{z})$ is the ponderomotive phase. The longitudinal distribution of the particles is represented by the term $\chi(z, \bar{z}) = N_{\bar{z}}(z, \bar{z})/n_0 \pi r_b^2 \Lambda$, where $N_{\bar{z}}(z, \bar{z})$ denotes the number of particles within a fraction of the radiation period allowing for a more accurate description of CSE effects when the current profile of the electron bunch varies significantly at the scale of the radiation period [5]. The source term is averaged over the associated subwavelength long beam segment Λ . \mathbf{F} is the filling factor. $\zeta_q(z, \bar{z})$ results from averaging the source term over the transverse

* ylurie@yosh.ac.il

gaussian density profile of the electron beam. For the case of a parallel plates (PP) waveguide it can be expressed by the analytical term:

$$\zeta_q(z, \bar{z}) = \frac{e^\xi}{\sqrt{8\kappa}\sigma_x(z)} \left\{ e^{\theta^2/4\eta} + e^{\theta^{*2}/4\eta} \right\} \quad (2)$$

with the parameters ξ , κ , η and θ defined in [5]. σ_x and σ_y are the rms transverse dimensions of the beam, determined by solving the beam envelope equations in terms of the longitudinal position z [4].

Due to the waveguide dispersion, slippage effects in short pulse waveguide FELs exhibit differences in comparison to open resonator FELs. The slippage length L_{sp} for the resonant radiation wavelength λ_r is defined as:

$$L_{sp} = N_w \lambda_r \left[1 - (k_{\perp q} / \beta_z \gamma_z k_w)^2 \right]^{1/2} \quad (3)$$

where N_w and $k_{\perp q}$ are the number of the wiggler periods and the cutoff wavenumber of the q 'th transverse mode, respectively.

The boundary conditions for the transverse modes are imposed by the resonator and can be formulated as follows:

$$u_{q''}^{(n+1)}(z = 0, t) = \rho^{(1)} \rho^{(2)} \times \sum_{q', q} \mathbf{P}_{q'' q'}^{(1)} \mathbf{P}_{q' q}^{(2)} e^{j\Phi_{q''}(\omega)} u_q^{(n)}(z = L_w, t - t_r) \quad (4)$$

where $u_q^{(n)}(L_w, t')$ denotes the complex amplitude of the q 'th mode at the exit of the interaction region at the pass number n and $t_r = L_c/v_{gr}$ is the cavity round-trip time. $\rho^{(i)}$ signifies reflectivity of the mirrors. $\mathbf{P}_{q'' q'}^{(i)}$ describes modes conversion, cavity losses and outcoupling.

The group velocity dispersion effects might influence the dynamics of the FEL amplification process in multiple round-trips. The inclusion of group velocity dispersion into the time domain model requires the solution of the second order wave equation [7]. In the presented model, the quadratic term associated with the group velocity dispersion is omitted in the waveguide dispersion relation as a consequence of SVEA. Instead, the dispersion is allowed for in an approximate manner in the model. Using a Fourier series expansion (FSE), the complex field amplitude $u_q(z, z')$ is expressed, at each pass, at the end of the FEL interaction in terms of longitudinal eigenmodes of the cold cavity with the respective $\omega_l = l \cdot 2\pi/t_r$ and $k_{zq}(\omega_l)$. Each l 'th longitudinal mode propagates with the own $k_{zq}(\omega_l)$ over the dispersive feedback section. Prior entering the interaction region, the field amplitudes of the longitudinal modes are summed (FSE⁻¹) to yield the updated $u_q(z = 0, t)$ which encompasses the effect of group velocity dispersion over the “drift” section in the preceding round-trip. Subsequently, starting the new round-trip, the procedure is repeated within the interaction region, after carrying out many integration steps in solving the first order wave equation as described in Eq. (1). Although the outlined algorithm makes use of the longitudinal cavity modes

in representing the complex field amplitude $u_q(z, z')$, it circumvents to reformulate the wave equation (1) for the amplitudes of the longitudinal modes and spares solving a large number of coupled axial mode equations.

Space-frequency model for FEL oscillators

Assuming a uniform cross-section resonator (usually a waveguide), the total electromagnetic field at every plane z can be expressed in the frequency domain as a sum of a set of transverse (orthogonal) eigenfunctions with profiles $\tilde{\mathcal{E}}_q(x, y)$ [2, 3]. At the beginning of a round-trip number n , each of the modes is assumed to have an initial amplitude $C_q^{(n)}(0, f)$ and the total field at $z = 0$ is given by:

$$\tilde{\mathbf{E}}^{(n)}(x, y, z = 0; f) = \sum_q C_q^{(n)}(0, f) \tilde{\mathcal{E}}_q(x, y) \quad (5)$$

At the end of the interaction region $z = L_w$, the field is:

$$\tilde{\mathbf{E}}^{(n)}(x, y, L_w; f) = \sum_q C_q^{(n)}(L_w, f) \tilde{\mathcal{E}}_q(x, y) e^{jk_{zq}(f)L_w} \quad (6)$$

The amplitude of the q 'th mode excited by the electron beam with current density $\tilde{\mathbf{J}}^{(n)}(x, y, z; f)$ is given by:

$$C_q^{(n)}(L_w, f) = C_q^{(n)}(0, f) - \frac{1}{2\mathcal{N}_q} \times \int_0^{L_w} \int \int \tilde{\mathbf{J}}^{(n)}(x, y, z; f) \cdot \tilde{\mathcal{E}}_q^*(x, y) e^{-jk_{zq}(f)z} dx dy dz \quad (7)$$

where the normalization of the mode amplitude is made via the complex Poynting vector power \mathcal{N}_q [3]. The spectral density of the energy flow after the interaction with the electron beam at the n 'th round-trip is:

$$\frac{d\mathcal{W}^{(n)}(L_w)}{df} = \sum_q \left| C_q^{(n)}(L_w, f) \right|^2 \frac{1}{2} \Re \{ \mathcal{N}_q \} \quad (8)$$

After a round-trip in the resonator of length L_c , the field at the entrance of the interaction region is [8]:

$$\begin{aligned} \tilde{\mathbf{E}}^{(n+1)}(x, y, z = 0; f) &= \sum_{q'} C_{q'}^{(n+1)}(0, f) \tilde{\mathcal{E}}_{q'}(x, y) = \\ &= \sum_{q'} \left[\sum_{q''} \rho_{q' q''} C_{q''}^{(n)}(L_w, f) \right] \tilde{\mathcal{E}}_{q'}(x, y) e^{jk_{zq'}(f)L_c} \end{aligned} \quad (9)$$

where $\rho_{q' q''}$ is a complex coefficient, expressing the inter-mode field reflectivity of transverse mode q'' to mode q' , due to scattering of the resonator mirrors or any other passive elements in the entire feedback loop. Scalar multiplication of both sides of Eq. (9) by $\tilde{\mathcal{E}}_{q'}^*(x, y)$, results in the initial mode amplitude:

$$C_q^{(n+1)}(0, f) = \sum_{q''} \rho_{qq''} C_{q''}^{(n)}(L_w, f) e^{jk_{zq}(f)L_c} \quad (10)$$

Table 1: Operational parameters of THz-FEL.

PARAMETER	THz FEL
Wavelength:	$\lambda \approx 1100 \mu\text{m}$
Beam energy:	$E_k = 10 \div 13 \text{ MeV}$
Energy spread:	$\sigma_e(\text{rms}) \approx 0.3\%$
Bunch charge:	$Q_b = 135 \text{ pC}$
Pulse length:	$\sigma_z(\text{rms}) = 1.0 \div 3.5 \text{ ps}$
Repetition rate:	23.6 MHz
Wiggler period:	$\lambda_w = 80 \text{ mm (hybrid.)}$
Wiggler:	$K(\text{rms}) = 0.8 \div 3.9$
Number of periods:	$N_w = 40$
Waveguide:	Rectangular ¹ ($38 \times 10 \text{ mm}^2$) or PP ² waveguide ($d = 10 \text{ mm}$)
Resonator round-trip length:	$\ell \simeq 6.35 \text{ m}$

which is required in equation (7) to solve the field excited in the consecutive round-trip. In the frequency domain, the total out-coupled radiation obtained at the oscillator output after N round-trips is composed of a summation of the circulated fields (6) inside the resonator:

$$\tilde{\mathbf{E}}_{out}(f) = \sum_q \Upsilon_q \sum_{n=0}^N C_q^{(n)}(L_w, f) \tilde{\mathcal{E}}_q(x, y) e^{+jk_{zq}(f)L_w} \quad (11)$$

where Υ_q is q th mode field transmission of the out-coupler. The energy spectrum of the electromagnetic radiation obtained at the output after N round-trips is given by:

$$\frac{d\mathcal{W}_{out}(N)}{df} = \sum_q \mathcal{T}_q \left| \sum_{n=0}^N C_q^{(n)}(L_w, f) \right|^2 \frac{1}{2} \Re \{ \mathcal{N}_q \} \quad (12)$$

where $\mathcal{T}_q = |\Upsilon_q|^2$ is the power transmission coefficient of mode q .

SIMULATIONS

To simplify the analysis, single transverse mode TE_{01} is assumed in the simulations. Operational parameters of the system is given in Table 1. Drive electron bunch consists from short $T_b = 7.2 \text{ ps}$ bunches with Gaussian longitudinal distribution and with an energy-phase correlation similar to the ones considered in [9, 10]. Figure 1 demonstrates spectrum of spontaneous emission obtained in the frequency domain by the WB3D code [3, 8]. The simulations were carried out with $N_p = 1000$ macroparticles; the resulted spectrum was then normalized to the number of electrons $N_e = Q_b/(N_p e)$ in the simulation (see [11] for details). The power of spontaneous emission is $P_{sp} =$

$W_{tot}^{(sp)}/\tau_{sp} \approx 5.5 \mu\text{W}$, where $W_{tot}^{(sp)} \approx 0.5 \text{ fJ}$ is the total energy flux of spontaneous emission found by integration of the spectrum, and $\tau_{sp} = L_w/v_{z0} - L_w/v_{gr} \approx 0.11 \text{ ns}$ is the slippage time.

The following results relate to FEL oscillator configuration, based on a train of bunches with repetition rate of about 23.6 MHz. Fig. 2 shows evolution of the bunching factor $b(z) = \overline{e^{jw_s t_i(z)}}$ along the wiggler as function of oscillator round-trip number. At the first round-trip, spontaneous emission takes place. At this stage, the intensity of the radiation is rather low and variations in the bunching factor are mainly due to the initial energy-time correlation in the electron bunch. At further round-trips, the emitted field causes additional bunching in the electron beam.

Evolution of the stored intracavity energy during the first round-trips is presented in Fig. 3. Fabry-Perot resonator lineshape is also drawn for the comparison. The free-spectral range is $FSR \approx \frac{1}{t_r} \approx 23.6 \text{ MHz}$, where $t_r = L_c/v_{gr} \approx 42.4 \text{ ns}$ is the round-trip time. The full-width half-maximum of the transmission peaks is given by $FWHM = \frac{FSR}{\mathcal{F}} \approx 0.65 \text{ MHz}$, where $\mathcal{F} = \frac{\pi \sqrt[4]{\mathcal{R}}}{1-\sqrt{\mathcal{R}}} = 36.0$ is the Finesse of the resonator ($\mathcal{R} = |\rho|^2 = 0.84$ is the total round-trip power reflectivity). The oscillator energy buildup is shown in Fig. 4.

Evolution of the radiation build-up process when the bunches with uncorrelated energy spread are injected was considered in the time domain model. Comparison of results of Fig. 4 and 5 reveals significant reduction of optical pulse energy at the last case. The difference might be explained by the enhancement of coherent emission due to energy-phase correlation, as described in [10].

CONCLUSIONS

In the paper we presented two approaches for simulating excitation and buildup of FEL radiation in an oscillator configuration. Using the models, a study of a FEL operated at the sub-millimeter wavelengths was carried out. The space-frequency model accounts for dispersion effects in the waveguide without approximations when radiation pulses are excited by a train of short electron bunches pro-

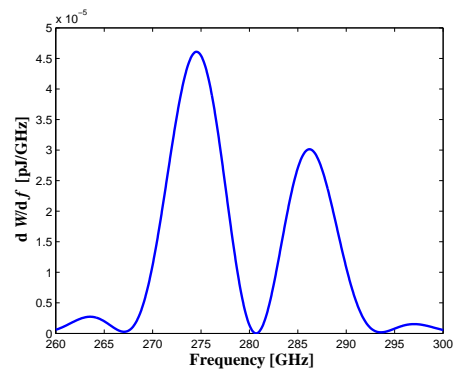


Figure 1: Spontaneous emission spectrum.

¹Simulations carried out in the time domain model.

²Simulations carried out in the space-frequency approach.

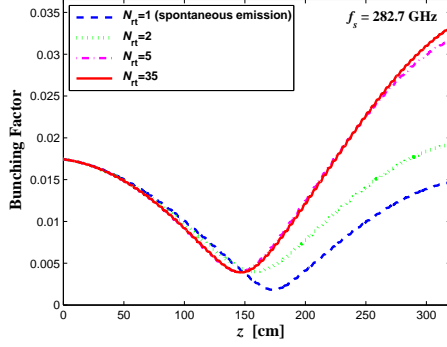


Figure 2: Evolution of the bunching factor along the wiggler for different oscillator round-trips.

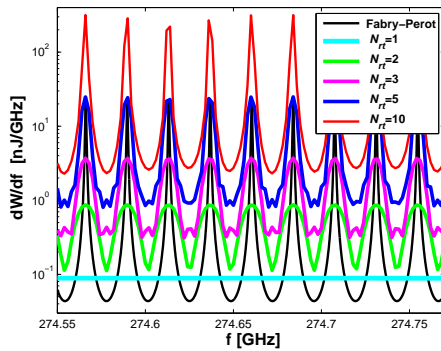


Figure 3: Oscillations build-up at the first round-trips.

duced by rf-linac.

REFERENCES

- [1] M.Tecimer et al., “A design study of a FIR/THz FEL for high magnetic field research”. Proc. of the 28th International FEL Conf., 2006, Berlin, Germany, p. 327.
- [2] Y. Pinhasi, V. Shterngartz and A. Gover, Phys. Rev. E **54** (1996) 6774.
- [3] Y. Pinhasi, Yu. Lurie, A. Yahalom, Phys. Rev. E **71** (2005) 036503.

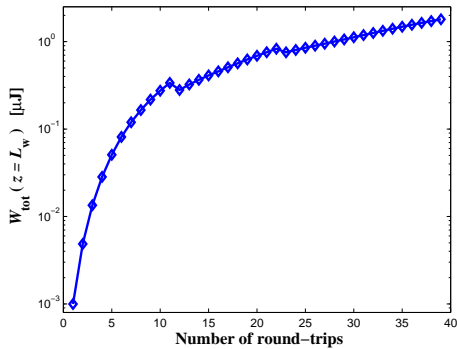


Figure 4: Evolution of the total stored intracavity energy.

- [4] G.H.C. van Werkhoven, Dissertation, TU Eindhoven (1995)
- [5] M. Tecimer, Dissertation, Tel Aviv University (2004)
- [6] L.R. Elias and J.C. Gallardo, Appl. Phys. B **31** (1983) 229.
- [7] N. S. Ginzburg et al., “Dispersion effects in short pulse waveguide FEL”. Proc. of the 28th International FEL Conf., 2006, Berlin, Germany, p. 378.
- [8] Y. Pinhasi, Y. Lurie, A. Yahalom, Nucl. Instr. Meth. Phys. Res. A **528** (2004) 62.
- [9] A. Doria et al., Phys. Rev. Lett. **80** (1998) 2841.
- [10] Yu. Lurie and Y. Pinhasi, Phys. Rev. ST Accel. Beams **10** (2007) 080703.
- [11] Y. Pinhasi, Yu. Lurie, Phys. Rev. E **65** (2002) 026501.

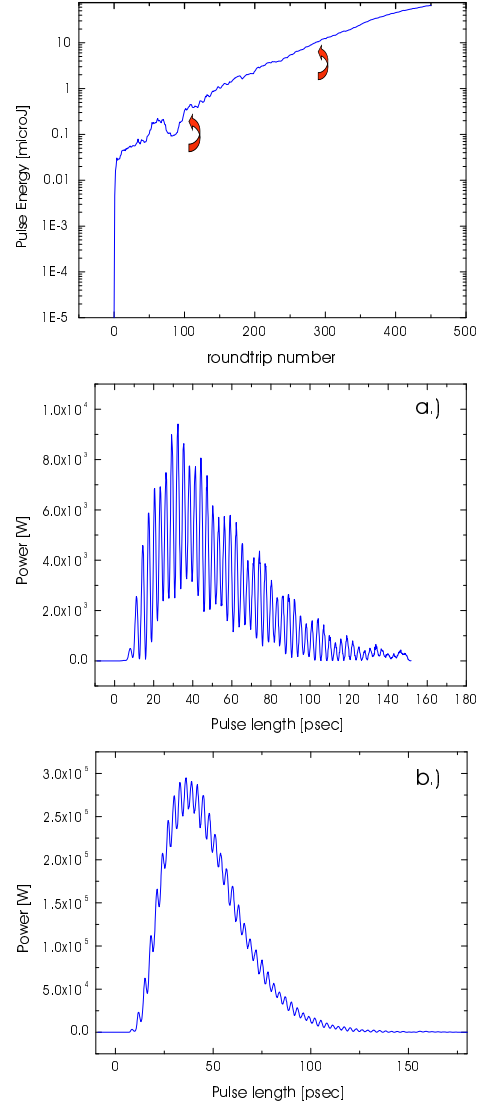


Figure 5: Evolution of the intracavity optical pulse energy for an uncorrelated Gaussian energy spread in the beam. The radiation power profile is shown at small signal gain (a) and at the beginning of the exponential gain (b) regimes, respectively.